CrossMark

Biosorption characteristics of *Ceratophyllum demersum* biomass for removal of uranium(VI) from an aqueous solution

Zheng-ji Yi[1,2] · **Jun Yao**[2] · **Mi-jia Zhu**[2] ·
Hui-lun Chen[2] · **Fei Wang**[2] · **Xing Liu**[1]

Abstract *Ceratophyllum demersum* was used to remove U(VI) from aqueous solution. Effects of various adsorption parameters such as pH, shaking time, initial U(VI) concentration, and temperature were investigated. The optimum pH for U(VI) removal was 5.0. Pseudo-first-order kinetic model and Langmuir isotherm model could best describe the adsorption process. The maximum monolayer adsorption capacity was 140.45 mg/g. Thermodynamic calculations suggested that the U(VI) adsorption process was spontaneous and exothermic. The amino, hydroxyl, and carbonyl groups on the algal surface could contribute to U(VI) adsorption. The present study suggested that *C. demersum* biomass could be an efficient biosorbent to remove U(VI) contaminants.

Keywords Uranium(VI) · Adsorption · *Ceratophyllum demersum* · Isotherm · Kinetics

Introduction

Uranium is a naturally occurring element and is generally distributed at low levels in many rocks, soils and sea water. In the past sixty years, uranium has been considered as one of the world's most important energy minerals. With the development of nuclear industry, increasing amounts of uranium-containing effluent produced annually from various nuclear-associated activities, such as uranium exploration and processing, manufacture of nuclear weapons, generation of nuclear power, and geological disposal of radioactive waste. Uranium is highly toxic and radioactive in the nuclear waste, and the bearable daily uptake of uranium is 0.6 µg/kg of body weight every day prescribed by World Health Organization (WHO) [1]. Because of its toxic effect and accumulation tendency throughout the food chain, contamination of the environment by hexavalent uranium(VI) and its health effects on human have been recently paid much attention.

To this day, some approaches, such as chemical precipitation [2], electrochemical precipitation [3], microbial reduction [4], membrane separation [5], solvent extraction [6], ion exchange [7], have been widely used for the removal of U(VI) from aqueous solution. But each method has its own disadvantages, such as high energy consumption, incomplete metal removal, limited tolerance to pH change, lack of metal selectivity, and production of harmful sludge requiring further treatment. Therefore, it is necessary for environmentalists to look for inexpensive and efficient remediation technology for removal of U(VI) from wastewater.

Aquatic plants, whatever living and dead, are heavy metal accumulators. Though floating macrophytes are considered promising biosorbents, submerged plants have been preferred for the removal of metals because they are fully submerged and have the ability to uptake metals directly from water bodies. In the past decades, biosorption of U(VI) onto certain algae has become a promising method for uranium removal. Compared with those conventional approaches, biosorption processes have several

✉ Jun Yao
yaojun@ustb.edu.cn

1 Key Laboratory of Functional Organometallic Materials of College of Hunan Province, School of Chemistry and Material Science, Hengyang Normal University, Hengyang 421008, China

2 School of Civil and Environmental Engineering, and National International Cooperation Base on Environment and Energy, University of Science and Technology Beijing, Xueyuan Road No. 30, Haidian District, Beijing 100083, China

advantages, such as low operation cost and no nutrient requirements. The metal biosorption mechanisms involve cell surface adsorption or precipitation, extracellular accumulation or precipitation and intracellular accumulation. So far, some experimental studies on U(VI) adsorption on various algae have been reported [8–11]. *Ceratophyllum demersum* is a submerged perennial macrophyte which normally grows with the base of its stem buried in sandy or silty substrates. It is considered to be a weed of waterways in many regions of the world because it is able to spread rapidly and invade a wide range of aquatic habitats. It also affects boating, fishing and other recreational activities. If *C. demersum* could be reaped and further utilized to remove radionuclide pollution, then we would realize the reclamation of wastes. Although previous study reported the effect of water hardness on the accumulation of uranium by living *C. demersum* [12], there was no literature reporting the use of dead *C. demersum* biomass for uranium sequestration. The application of dead biomass in heavy metal uptake is better because there are no toxicity consideration, no requirement of growth media and it is easy to remove pollutants from the biomass and regenerate them.

In the present work, the goal of the experiments was to examine the ability of dead *C. demersum* to uptake uranium. The U(VI) biosorption characteristics of *C. demersum* were investigated regarding contact time, pH, temperature, and initial U(VI) concentration via a series of batch tests. The relative adsorption isotherms, kinetics, and thermodynamics were also discussed.

Experimental

Materials and reagents

C. demersum biomass used in the present study was purchased from Honghu Liangshui Aquatic Plant Co. Ltd., Jingzhou, China. The fresh biomass was rinsed thoroughly with running water to remove silt, sand, diatoms, and other epiphytic organisms. Then the biomass was dried under sunlight for three days and subsequently dewatered at 80 °C for 24 h in a drying oven. The dried biomass was pulverized into fine powder and allowed to pass through an 80 mesh opening size sieve. The treated biomass was placed in a desiccator for subsequent use in the biosorption experiments.

A stock solution of U(VI) (1000 mg/L) was prepared by dissolving 1.1792 g of U_3O_8 in a mixture of HCl and H_2O_2 [13]. U_3O_8 was courtesy of the School of Nuclear Resources and Nuclear Fuel Engineering of the University of South China. The other required concentrations (50–300 mg/L) were obtained by diluting the

aforementioned standard U(VI) stock solution with distilled water. All other chemical reagents were analytical grade, commercially available, and used as received without any further treatment.

Uranium adsorption experiments

Generally, 0.14 g of adsorbents were added to a series of 250 mL stoppered conical flasks containing 100 mL of uranium solution with the desired initial U(VI) concentrations (50–300 mg/L). The pH of the solutions was adjusted when required by adding HCl (1.0 or 0.1 M) or NaOH (1.0 or 0.1 M) and by using a pH meter. Then, these flasks were shaken on a reciprocal rotary shaker at 140 r/min for specified durations at the desired temperatures (298–318 K). Supernatant samples were collected at suitable time intervals, centrifuged at $5000 \times g$ for 5 min, and analyzed for residual U(VI) concentrations by using the standard method described by the method described as [14]. The U(VI) removal efficiency (Ad%) and U(VI) adsorption capacity (Q) can be determined according to the following equations:

$$Ad\% = \frac{C_0 - C_t}{C_0} \times 100, \tag{1}$$

$$Q_t = \frac{(C_0 - C_t) \times V}{W}, \tag{2}$$

$$Q_e = \frac{(C_0 - C_e) \times V}{W}, \tag{3}$$

where Ad% is the U(VI) removal efficiency; Q_e and Q_t are the U(VI) adsorption capacity (mg/g) at equilibrium and at time t (min), respectively; C_0, C_t, and C_e are the initial U(VI) concentration, liquid-phase U(VI) concentration at time t, and equilibrium U(VI) concentration (mg/L), respectively; V is the volume of the aqueous solution (L); and W is the mass of the adsorbent (g). All the experiments were conducted in triplicate, and the arithmetic mean values of the calculations were recorded. Blank experiments were conducted to ensure that no adsorption occurred on the walls of the glassware.

Adsorption kinetics fitting

Kinetic models are usually employed to describe the rate-determining step of the adsorption process. Two commonly used kinetic models, namely, pseudo-first-order and pseudo-second-order models, were selected to analyze the kinetic data and to understand the rate-determining step of U(VI) adsorption onto *C. demersum* biomass.

The pseudo-first-order equation is a simple kinetic model describing the kinetic process of liquid–solid phase

sorption [15], and its linear formula can be written as follows:

$$\ln(Q_e - Q_t) = \ln Q_e - k_1 t, \tag{4}$$

where k_1 is the rate constant of the pseudo-first-order sorption (min^{-1}). Evidently, k_1 can be calculated from the slope of the plot of $\ln(Q_e - Q_t)$ versus t.

The pseudo-second-order model based on the adsorption equilibrium capacity can be expressed in the following linear form [16]:

$$\frac{t}{Q_t} = \frac{t}{Q_e} + \frac{1}{k_2 Q_e^2}, \tag{5}$$

where k_2 is the rate constant of pseudo-second-order adsorption [g/(mg min)]. Evidently, Q_e and k_2 can be determined experimentally by plotting t/Q_t versus t and further linear regression analysis.

Adsorption isotherm fitting

Three extensively used adsorption isotherm models, namely, Langmuir, Freundlich, and Temkin, were selected to correlate the experimental data and to describe the adsorption isotherms exactly. The deviation between experimentally observed and theoretically calculated data can be described by the square of the correlation coefficient (R^2).

The Langmuir model is based on the assumptions of adsorption homogeneity, such as uniformly energetic adsorption sites, monolayer surface coating, and no interactions among adsorbate molecules in neighboring sites [17]. The linear Langmuir equation can be written as follows:

$$\frac{C_e}{Q_e} = \frac{1}{Q_{max}} C_e + \frac{1}{b Q_{max}}, \tag{6}$$

where Q_{max} is the maximum possible amount of metals adsorbed per unit of weight of adsorbent (mg/g) and b is a constant associated with the affinity of binding sites for metals (L/mg). Q_{max} and b can be determined from the plot of C_e/Q_e versus C_e. Based on further analysis of the Langmuir equation, the Langmuir adsorption isotherm can be described by using an equilibrium parameter (R_L) calculated by using the following equation:

$$R_L = \frac{1}{1 + b \times C_0}, \tag{7}$$

where the R_L value indicates whether the adsorption process is irreversible $(R_L = 0)$, favorable $(0 < R_L < 1)$, linear $(R_L = 1)$, or unfavorable $(R_L > 1)$.

The Freundlich isotherm may be suitable for nonideal uptake onto heterogeneous surfaces involving multilayer adsorption [18]. The linear Freundlich equation can be expressed as follows:

$$\ln Q_e = \ln K_F + \frac{1}{n} \ln C_e, \tag{8}$$

where K_F is the Freundlich constant depicting the adsorption capacity of the adsorbent $((\text{mg/g})(\text{L/mg})^{1/n})$ and n is the Freundlich exponent depicting adsorption intensity (dimensionless). K_F and n can be determinded from the plot of $\ln Q_e$ versus $\ln C_e$.

The Temkin model assumes a linear decrease in heat of adsorption along with surface coverage [19], and its linear form is written as follows:

$$Q_e = a \ln K_T + a \ln C_e, \tag{9}$$

where K_T is an equilibrium parameter corresponding to the maximum binding energy (L/g) and a is a dimensionless constant related to the temperature and adsorption system. The Temkin isotherm considers the interaction between adsorbent and adsorbate and is based on the assumption that the free energy of adsorption is a function of the surface coverage.

Thermodynamic parameters of biosorption

The thermodynamic parameters could be determined by using the equilibrium constant or distribution coefficient, K_d, which depends on temperature. The change in free energy (ΔG^0), enthalpy (ΔH^0), and entropy (ΔS^0) related to the adsorption process can be calculated by using the following three equations [20]:

$$\Delta G = -RT \ln K_d, \tag{10}$$

$$K_d = \frac{Q_e}{C_e}, \tag{11}$$

$$\ln K_d = \frac{\Delta S^0}{R} - \frac{\Delta H^0}{RT}, \tag{12}$$

where R is the universal gas constant $(8.314 \text{ J mol}^{-1} \text{ K}^{-1})$ and T (K) is the absolute temperature. According to Eq. (12), the parameters ΔH^0 and ΔS^0 can be calculated from the slope and intercept of the plot of $\ln K_d$ against $1/T$.

Characterization methods

The sample of *C. demersum* (0.14 g) with exposure to 100 mL of 150 mg/L U(VI) solution at pH 5.0 for 1 h was centrifuged $(5000 \times g, 5 \text{ min})$ to remove all supernatants. Then the precipitation was further dehydrated by vacuum freeze drying. The samples before and after U(VI) biosorption were characterized using the following two instrumental analyses. FTIR spectroscopy was determined by a NICOLET iS10 (Thermo Scientific) within

$500{-}4000\ \text{cm}^{-1}$ and by using KBr pellets. The surface morphology of *C. demersum* surface was determined by SEM (Model S-4800 Hitachi, Tokyo, Japan). The samples were gold coated before SEM observation. XPS (Thermo ESCALAB 250, USA) with a monochromatic Al Kα X-ray beam (energy = 1486.5 eV and power = 150 W) was adopted to determine the elementary composition and relative uranium content on the surface of *C. demersum*. The XPS spectra were recorded in the fixed analyzer transmission mode with a pass energy of 20 eV and a step size of 0.1 eV and obtained at 8×10^{9} Pa.

Results and discussion

Contact time dependence of U(VI) adsorption and kinetics study

Figure 1 gives the time course profiles of U(VI) uptake at three different temperatures. Notably, a considerable amount of U(VI) was quickly adsorbed in the first 60 min. Subsequently, the U(VI) adsorption slightly slowed down and eventually reached equilibrium within 120 min for
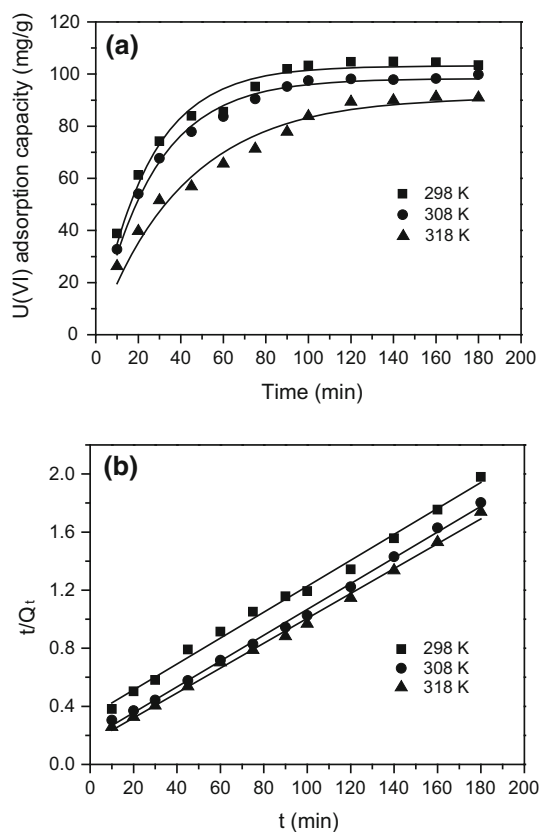

Fig. 1 a Effect of time on U(VI) adsorption onto *C. demersum* and pseudo-first-order kinetic fit; b plot of pseudo-second-order kinetic fit (temperature = 298 K; pH = 5.0; U(VI) concentration = 180 mg/L; *C. demersum* dosage = 1.4 g/L (w/v); solution volume = 100 mL)

each examined temperature. The rapid U(VI) adsorption at the beginning could be due to the greater concentration gradient and more available sites for adsorption. After some time, the residual vacant surface sites could be hard to occupy due to repulsive forces between the solute molecules of the solid and bulk phase. Therefore, a contact time of 120 min was adopted for the subsequent experiments to ensure that adsorption equilibrium was reached.

The kinetic parameters for pseudo-first-order and pseudo-second-order models at three different temperatures are given in Table 1. Evidently, the theoretical Q_e values calculated from the pseudo-second-order kinetic model were not close to the experimental values and the R^2 values were lower than 0.99 (Table 1), indicating that the U(VI) uptake could not follow the pseudo-second-order model. However, for all temperatures, the R^2 values for pseudo-first-order kinetic model were found to be greater than those of pseudo-second-order model and the calculated Q_e values derived from pseudo-first-order kinetic model were much closer to the experimental data. According to the results, the adsorption of U(VI) onto *C. demersum* could be described by the pseudo-first-order kinetic model. The result differed from biosorption of U(VI) with *Dictyopteris polypodioides* brown alga [11] and *Catenella repens* red alga [8], which followed pseudo-second-order kinetics.

pH dependence of U(VI) adsorption

The pH is an important parameter for the metal adsorption because it controls the charge of the adsorbent surface as well as the existence in various forms of the adsorbate in solution. In this study, the adsorption experiments were carried out in the initial pH range of 2.0–7.0 (Fig. 2). It is evident that the U(VI) adsorption capacity increased with the increase of pH value, and achieved a maximum at pH 5.0. Generally speaking, the surface charge of *C. demersum* could be modified with the change of solution pH. At very acidic pH, uncomplexed uranyl (UO_2^{2+}) was dominant [21], and the adsorption sites of *C. demersum* became positively charged due to the protonation reaction, exhibiting the cationic character. The repelling force between the cationic surface and uranyl cations was unfavorable to U(VI) biosorption, resulting in the low U(VI) removal efficiency. Along with the increase of pH, the functional groups on the surface of *C. demersum* are progressively deprotonated, forming a negative charge state. The attractive forces between the anionic surface sites and cationic uranyl ions promoted the U(VI) removal.

However, the U(VI) adsorption capacity turns to decrease with the increased pH value beyond 5.0. It can be explained that with the increase of the concentration of hydroxyl, most of U(VI) would form highly negative charged complexes with OH^- and CO_3^{2-} (came from the

Table 1 Kinetic parameters of U(VI) adsorption onto *C. demersum*

Temperature	$Q_{e, exp}$ (mg/g)	Pseudo-first-order			Pseudo-second-order		
		k_1 (min^{-1})	Q_{e1} (mg/g)	R^2	k_2 (g mg^{-1} min^{-1})	Q_{e2} (mg/g)	R^2
298 K	104.38	0.0411	103.14	0.9904	118.98	4.41×10^{-4}	0.9821
308 K	98.51	0.0375	98.28	0.9958	114.95	3.97×10^{-4}	0.9885
318 K	90.36	0.0242	91.34	0.9897	112.84	2.29×10^{-4}	0.9835
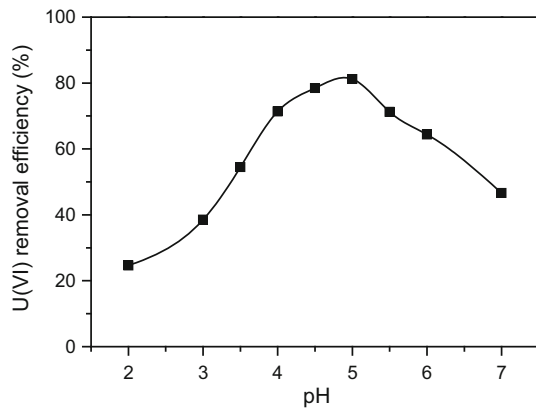
Fig. 2 Effect of pH on U(VI) adsorption onto *C. demersum*, (temperature = 298 K; contact time = 120 min; U(VI) concentration = 180 mg/L; *C. demersum* dosage = 1.4 g/L (w/v); solution volume = 100 mL)

dissolution of CO_2 in air) such as $(UO_2)_2CO_3(OH)_3^-$, $UO_2(CO_3)_2^{2-}$, $UO_2(CO_3)_3^{4-}$ [22]. The repulsion between the anionic surface and negative charged uranyl complexes led to the decrease of U(VI) removal. According to the above discussion, the optimum pH value is 5.0.

Influence of initial U(VI) concentration and adsorption isotherm study

Figure 3 shows the experimental results of adsorption of U(VI) onto *C. demersum* at various concentrations. The adsorption capacity of adsorbent increased from 33.09 to 131.23 mg/g when the initial concentration of U(VI) increased from 50 to 300 mg/L (Fig. 3a), which could be interpreted that the initial concentration gradients give an important driving force to overcome the mass transfer resistance of uranium between the aqueous and solid phase. Adsorption isotherm provides the most critical information on how the adsorbate molecules distribute between the liquid phase and solid phase while adsorption process reaches equilibrium. The adsorption data over the initial U(VI) concentration range mentioned above were fitted with three isotherm models including Freundlich, Langmuir and Temkin models in order to explain the adsorption

mechanism (Fig. 3b–d). The corresponding isotherm parameters and R^2 values are summarized in Table 2. Based on the analysis of the R^2 values of the above three models, it is found that the adsorption onto *C. demersum* could be best characterized by the Langmuir model and the monolayer maximum capacity was 140.45 mg/g. Our result is similar to the previous study on the biosorption of U(VI) by *Padina* sp. algae biomass [9] and brown alga *Cystoseira indica* [23], both of which can be described by Langmuir model. By comparison with other biosorbents, the maximum U(VI) biosorption capacity of *C. demersum* (140.45 mg/g) is higher than 6.789 mg/g of ethylenediamine-modified biomass of *Aspergillus niger* [24], 29.412 mg/g of tea waste [25], 94.30 mg/g of magnetic Schiff base (ferroferric oxide/schiff base composite) [18] and 125 mg/g of oxine functionalized magnetic Fe_3O_4 particles [26]. In addition, R_L values were between 0 and 1 for all the studied U(VI) concentrations, which revealed that *C. demersum* was a favorable biosorbent for U(VI).

Adsorption thermodynamics study

The thermodynamic parameters were derived from the experimental results obtained at various temperatures but fixed initial U(VI) concentration of 180 mg/L. The values of ΔH^0 and ΔS^0 calculated from the slope and intercept of $\ln K_d$ against $1/T$ were −23.64 kJ/mol and −69.91 J/mol/K, respectively (Fig. 4). The negative ΔS^0 value can be explained by the increased degree of orderliness, reflecting the higher affinity of the *C. demersum* surface for U(VI). The negative ΔH^0 value indicated an exothermic nature of the sorption process. Besides, enthalpy rather than entropy appeared to be the driving force of biosorption from the thermodynamic viewpoint. Furthermore, the ΔG^0 values at different temperatures were calculated and shown in Table 3. The negative ΔG^0 values indicated that the adsorption reaction was spontaneous. The ΔG^0 value becomes less negative with increasing temperature, which implied that the biosorption process is more favorable at lower temperatures. Hence, the biosorption of U(VI) by *C. demersum* was an entropically unfavorable, enthalpy driven spontaneous process and exothermic in nature.
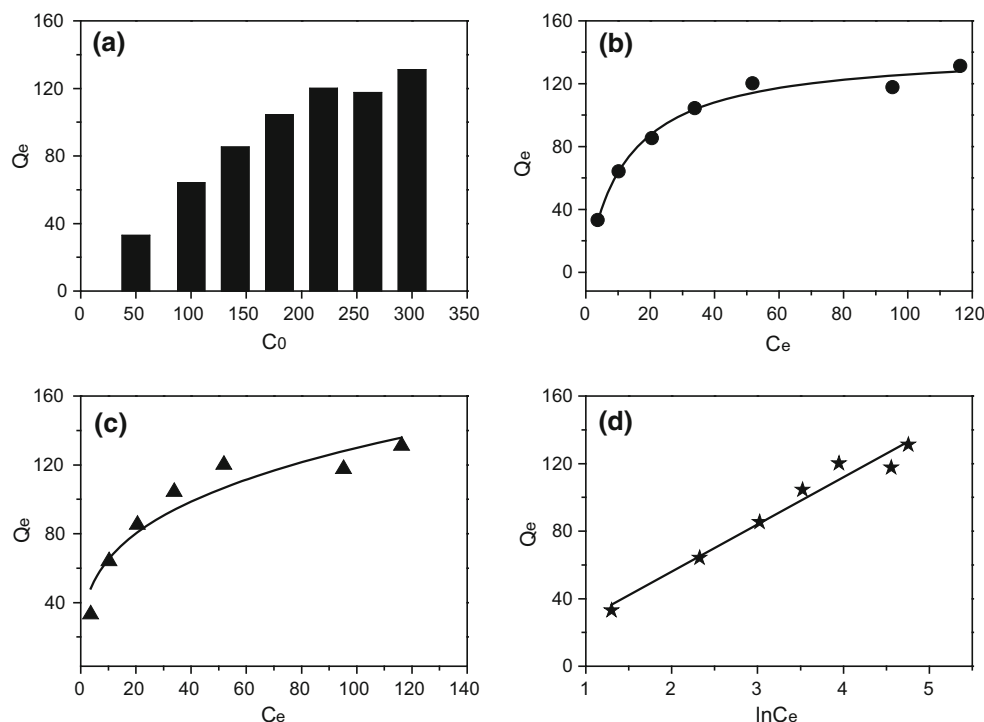
Table 2 Isotherm parameters for the adsorption of U(VI) onto *C. demersum*

Model	Parameter	Value
Langmuir	Q_{max} (mg/g)	140.45
	b	0.0828
	R^2	0.9928
	R_L	0.0195–0.0387
Freundlich	K_F (mg$^{(1-n)}$ g L^{-1})	24.31
	n	2.6476
	R^2	0.9035
Temkin	K_T	1.0043
	a	27.95
	R^2	0.9613
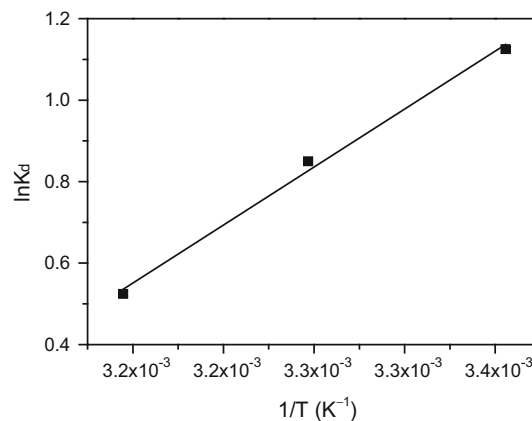
Fig. 4 Plot of $\ln K_d$ against $1/T$ for the calculation of the thermodynamic parameters

FTIR analysis of C. demersum

The FTIR spectra of *C. demersum* before and after U(VI) adsorption are given in Fig. 5. As for the FTIR spectrum of raw *C. demersum* without contacting U(VI), the weak absorption shoulder appearing around 3290.93 cm^{-1} might correspond to the O–H and N–H stretching vibrations and implied that the surface of *C. demersum* was rich in hydroxyl (–OH) and amino (–NH$_2$) groups. The peak detected at 2919.70 could be related to the C–H stretching vibration of methylene (–CH$_2$–) which serve as the structural components of the alga. The peak at 1631.97 cm^{-1} could be attributed to the carbonyl (C=O) stretching

vibration. The intensive peak at 1023.05 cm^{-1} could be assigned to the C–OH stretching vibration.

As for the FTIR spectrum of the alga sample with exposure to U(VI), the peak position observed at
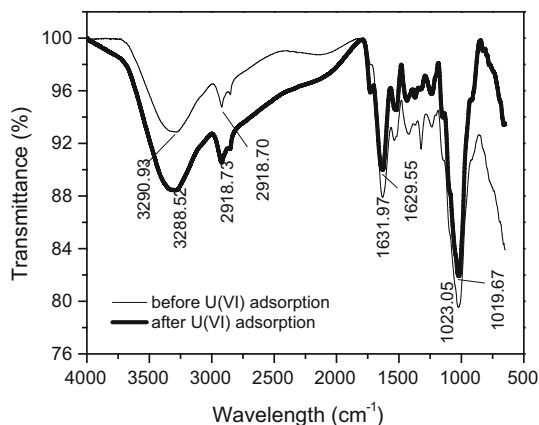
Table 3 Thermodynamic parameters for adsorption onto *C. demersum*

ΔH^0 (kJ mol^{-1})	ΔS^0 (J mol^{-1} K^{-1})	ΔG^0 (kJ mol^{-1})		
		298 K	308 K	318 K
−23.64	−69.91	−2.79	−2.11	−1.41

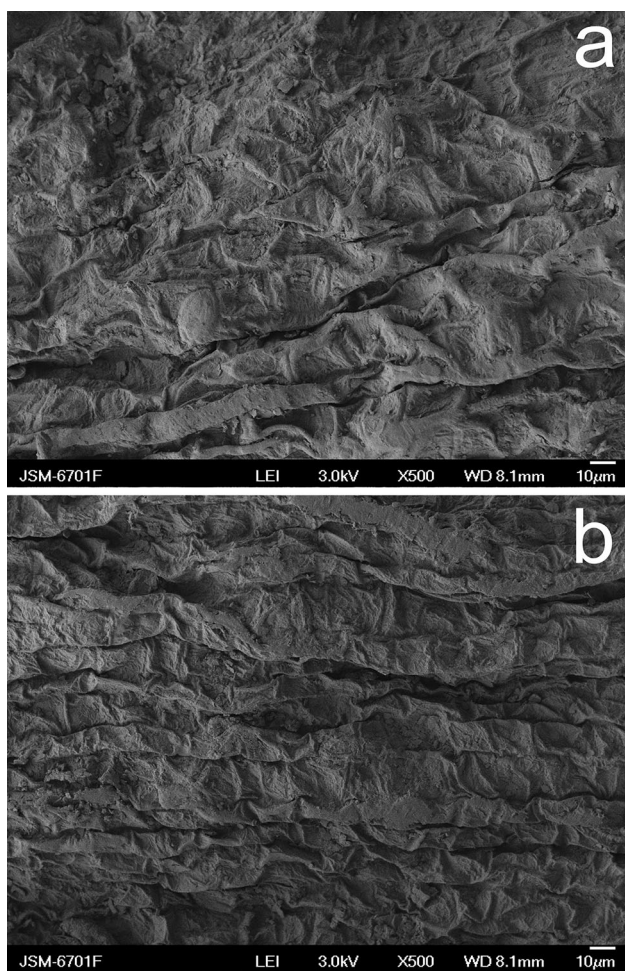**Fig. 5** FTIR spectra of *C. demersum*: **a** before U(VI) adsorption; **b** after U(VI) adsorption

Fig. 6 SEM micrographs of *C. demersum*: **a** before U(VI) adsorption, magnification ×500; **b** after U(VI) adsorption, magnification ×500

Fig. 7 XPS analysis of *C. demersum*: **a** before U(VI) adsorption; **b** after U(VI) adsorption)

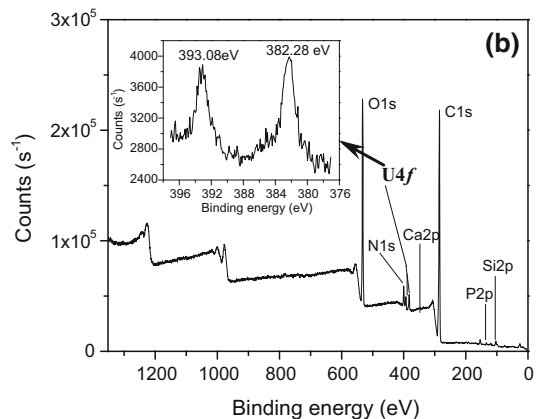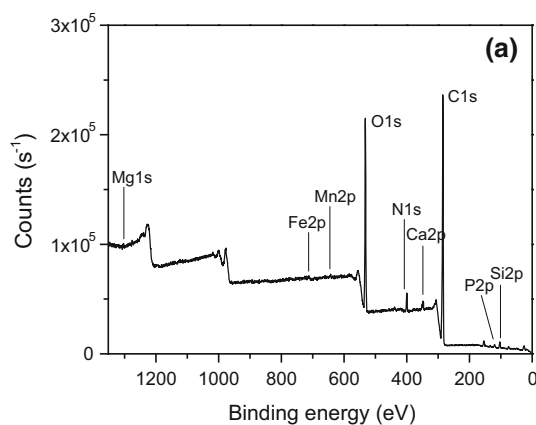2918.70 cm^{-1} remained nearly unchanged, which indicated that methylene contributed little to U(VI) adsorption. In contrast, the peaks at 3290.93, 1631.97 and 1023.05 cm^{-1} shifted to 3288.52, 1629.55 and 1019.67 cm^{-1}, respectively. Meanwhile, the peak intensity of these peaks also varied significantly after U(VI) biosorption. In summary, the changes of peak position and intensity demonstrated that there were strong coordination interactions between U(VI) ions and hydroxyl, amino and carbonyl functional groups on the algal surface, which could play a big role in the U(VI) biosorption. Biosorption included adsorption (accumulation of substances at the surface or interface) as well as absorption (penetration of atoms or molecules of one phase forming a solution with a second phase). Both living and dead biomasses have metal biosorption ability in which ligands are involved. The algal matrix contains various complex structural polysaccharides. Biosorption is ascribed mainly to the algal cell wall, where electrostatic attraction and coordination both serve important functions [27]. Gunther et al. [28] reported that the uptake of uranium by *Chlorella regularis* is dependent not only on the physical adsorption on the cell surface, but also on the electrostatic attraction and chemical adsorption of uranyl ions through complex formation with cellular ligands. Their results are very similar to ours.

Table 4 XPS atomic concentration (in percentage) of relevant chemical elements in *C. demersum* sample, before and after U(VI) uptake

Biomass sample	C	O	N	Si	Fe	Ca	P	Mg	Mn	U
Before U(VI) uptake	70.17	21.57	4.21	2.1	0.27	0.77	0.35	0.09	0.45	ND
After U(VI) uptake	68.87	22.66	5.01	2.67	ND	ND	0.64	ND	ND	0.15

SEM analysis of *C. demersum*

The morphologies of *C. demersum* before and after exposure to U(VI) were characterized via SEM observation (Fig. 6). Notably, the surface of raw *C. demersum* was rough and irregular, and many depressions could be clearly observed (Fig. 6a). Because the diameter of the U(VI) ion was picometer-scale (ca. 92 pm), these micrometer-scale concaves on the algal surface could hold substantial uranyl ions. In contrast, after exposure to U(VI), the surface of *C. demersum* became relatively regular and assumed a specific texture with many bending stripe ribbons arranged side by side. By comparing Fig. 6a with b, it was found that *C. demersum* could change its own surface structure to promote U(VI) binding.

XPS analysis of *C. Demersum*

To identify the interaction mechanism between U(VI) and *C. demersum*, the wide-scan survey XPS spectra and U4*f* narrow-scan XPS spectra for the alga before as well as after U(VI) uptake were recorded (Fig. 7). Besides, the atomic concentrations of relevant chemical elements in the *C. demersum* sample with and without exposure to U(VI) were also analyzed (Table 4). Obviously, *C. demersum* contained three major nonmetal elements (C, O, and N), three minor nonmetal elements (Si and P), and three major metal elements (Ca, Fe and Mn) (Fig. 7; Table 4). Besides, U element was not detected in the structural constituents of *C. demersum*.

However, the uranium signal was clearly found after U(VI) biosorption. The primary U4*f* peaks ascribed to U(VI) lay in 382.38 eV (4*f*7/2) and 393.08 eV (4*f*5/2) (Fig. 7b). The two binding energy values could be associated with the bond between U(VI) ion and hydroxyl and amino functional groups [20, 29]. In particular, the atomic concentrations of Fe, Ca, Mn and Mg fell under the limit of detection along with the adsorption of uranium onto the *algal* surface, indicating that ion exchange between uranium and these metals (Fe, Ca, Mn and Mg) could occur. From the XPS and FTIR analyses, two possible biosorption mechanisms, coordination and electrostatic attraction, might be involved in the biosorption process.

Conclusions

In this study, the use of *C. demersum* in the effective removal of U(VI) was revealed and new insights into the binding mechanism were gained. Some parameters such as contact time, solution pH, and metal concentration, were also investigated. The alga had a maximum U(VI) removal at pH 5.0. The adsorption process could be characterized by the pseudo-first-order kinetic model, and the adsorption isotherm fitted very well to the Langmuir equation. The FIIR and XPS analyses showed that the adsorption of U(VI) onto the *C. demersum* was mainly through coordination and electrostatic attraction. The regeneration and reuse of the biosorbent and fixed-bed column adsorption required further study.

References

1. Zhang S, Shu XW, Zhou Y, Huang L, Hua DB (2014) Highly efficient removal of uranium(VI) from aqueous solutions using poly(acrylic acid)-functionalized microspheres. Chem Eng J 253:55–62
2. Mellah A, Chegrouche S, Barkat M (2007) The precipitation of ammonium uranyl carbonate (AUC): thermodynamic and kinetic investigations. Hydrometallurgy 85(2–4):163–171
3. Prasadaao TR, Metilda P, Gladis JM (2006) Preconcentration techniques for uranium(VI) and thorium(IV) prior to analytical determination-an overview. Talanta 68(4):1047–1064
4. Newsome L, Morris K, Trivedi D, Atherton N, Lloyd JR (2014) Microbial reduction of uranium(VI) in sediments of different lithologies collected from Sellafield. Appl Geochem 51:55–64
5. Ambashta RD, Sillanpaa MET (2011) Membrane purification in radioactive waste management: a short review. J Environ Radioact 105:76–84
6. Kumar JR, Kim JS, Lee JY, Yoon HS (2011) A brief review on solvent extraction of uranium from acidic solutions. Sep Purif Rev 40(2):77–125
7. Stucker V, Ranville J, Newman M, Peacock A, Cho J, Hatfield K (2011) Evaluation and application of anion exchange resins to measure groundwater uranium flux at a former uranium mill site. Water Res 45(16):4846–4876

8. Bhat SV, Melo JS, Chaugule BB, D'Souza SF (2011) Biosorption of uranium(VI) from aqueous solutions by Ca-pretreated *Cystoseira indica* alga: Breakthrough curves studies and modeling. J Hazard Mater 189(1–2):141–149

9. Khani MH (2011) Statistical analysis and isotherm study of uranium biosorption by *Padina* sp. algae biomass. Environ Sci Pollut Res 18(5):790–799

10. Lee KY, Kim KW, Baek YJ, Chung DY, Lee EH, Lee SY, Moon JK (2014) Biosorption of uranium(VI) from aqueous solution by biomass of brown algae *Laminaria japonica*. Water Sci Technol 70(1):136–143

11. Bampaiti A, Yusan S, Aytas S, Pavlidou E, Noli F (2016) Investigation of uranium biosorption from aqueous solutions by Dictyopteris polypodioides brown algae. J Radioanal Nucl Chem 307(2):1335–1343

12. Markich SJ (2013) Water hardness reduces the accumulation and toxicity of uranium in a freshwater macrophyte (*Ceratophyllum demersum*). Sci Total Environ 443:582–589

13. Zhang ZB, Yu XF, Cao XH, Hua R, Li M, Liu YH (2014) Adsorption of U(VI) from aqueous solution by sulfonated ordered mesoporous carbon. J Radioanal Nucl Chem 301(3):821–830

14. Xie SB, Zhang C, Zhou XH, Yang J, Zhang XJ, Wang JS (2009) Removal of uranium(VI) from aqueous solution by adsorption of hematite. J Environ Radioact 100(2):162–166

15. Song J, Kong H, Jang J (2011) Adsorption of heavy metal ions from aqueous solution by polyrhodanine-encapsulated magnetic nanoparticles. J Colloid Interface Sci 359(2):505–511

16. Tan LC, Liu Q, Jing XY, Liu JY, Song DL, Hu SX, Liu LH, Wang J (2015) Removal of uranium(VI) ions from aqueous solution by magnetic cobalt ferrite/multiwalled carbon nanotubes composites. Chem Eng J 273:307–315

17. Solgy M, Taghizadeh M, Ghoddocynejad D (2015) Adsorption of uranium(VI) from sulphate solutions using Amberlite IRA-402 resin: Equilibrium, kinetics and thermodynamics study. Ann Nucl Energy 75:132–138

18. Zhang XF, Jiao CS, Wang J, Liu Q, Li RM, Yang PP, Zhang ML (2012) Removal of uranium(VI) from aqueous solutions by magnetic Schiff base: kinetic and thermodynamic investigation. Chem Eng J 198–199:412–419

19. Yang SK, Tan N, Yan XM, Chen F, Lin YC (2013) Adsorption of thorium(IV) from aqueous solution by non-living biomass of mangrove endophytic fungus Fusarium sp. #ZZF51. J Radioanal Nucl Chem 298(2):827–833

20. Ai L, Luo XG, Lin XY, Zhang SZ (2013) Biosorption behaviors of uranium(VI) from aqueous solution by sunflower straw and insights of binding mechanism. J Radioanal Nucl Chem 298(3):1823–1834

21. Bai J, Fan FL, Wu XL, Tian W, Zhao L, Yin XJ, Fan FY, Li Z, Tian LL, Wang Y, Qin Z, Guo JS (2013) Equilibrium, kinetic and thermodynamic studies of uranium biosorption by calcium alginate beads. J Environ Radioact 126:226–231

22. Ortaboy S, Atun G (2014) Kinetics and equilibrium modeling of uranium(VI) sorption by bituminous shale from aqueous solution. Ann Nucl Energy 73:345–354

23. Keshtkar AR, Mohammadi M, Moosavian MA (2015) Equilibrium biosorption studies of wastewater U(VI), Cu(II) and Ni(II) by the brown alga *Cystoseira indica* in single, binary and ternary metal systems. J Radioanal Nucl Chem 303(1):363–376

24. Ding DX, Xin X, Li L, Hu N, Li GY, Wang YD, Fu PK (2014) Removal and recovery of U(VI) from low concentration radioactive wastewater by ethylenediamine modified biomass of *Aspergillus niger*. Water Air Soil Pollut 225:2206

25. Li XY, Li FB, Jin Y, Jiang CJ (2015) The uptake of uranium by tea wastes investigated by batch, spectroscopic and modeling techniques. J Mol Liq 209:413–418

26. Tan LC, Wang J, Liu Q, Sun YB, Zhang HS, Wang YL, Jing XY, Liu JY, Song DL (2015) Facile preparation of oxine functionalized magnetic Fe_3O_4 particles for enhanced uranium(VI) adsorption. Colloids Surf, A 466:85–91

27. Singhal RK, Basu H, Pimple MV, Manisha V, Basan MKT, Reddy AVR (2013) Spectroscopic determination of U(VI) species sorbed by the *Chlorella* (*Chlorella pyrenoidosa*) fresh water algae. J Radioanal Nucl Chem 298(1):587–592

28. Gunther A, Raff J, Geipel G, Bernhard G (2008) Spectroscopic investigations of U(VI) species sorbed by the green algae *Chlorella vulgaris*. Biometals 21(3):333–341

29. Nancharaiah YV, Joshi HM, Mohan TVK, Venugopalan VP, Narasimhan SV (2006) Aerobic granular biomass: a novel biomaterial for efficient uranium removal. Curr Sci 91(4):503–509